J Bionic Eng 18 (2021) 375–386
DOI: https://doi.org/10.1007/s42235-021-0027-x
Journal of Bionic Engineering
http://www.springer.com/journal/42235

An Optimised Surface Structure for Passive, Unidirectional Fluid Transport Bioinspired by True Bugs

Sebastian Lifka[1*], Florian Hischen[1], Johannes Heitz[2], Werner Baumgartner[1]

1. *Institute of Biomedical Mechatronics*, *Johannes Kepler University Linz*, *Altenberger Straße* 69, 4040 *Linz*, *Austria*
2. *Institute of Applied Physics*, *Johannes Kepler University Linz*, *Altenberger Straße* 69, 4040 *Linz*, *Austria*

Abstract

Some true bug species use droplet-shaped, open-capillary structures for passive, unidirectional fluid transport on their body surface in order to spread a defensive fluid to protect themselves against enemies. In this paper we investigated if the shape of the structures found on bugs (bug-structure) could be optimised with regard to better performance in unidirectional fluid transportation. Furthermore, to use this kind of surface structure in technical applications where fluid surface interaction occurs, it is necessary to adapt the structure geometry to the contact angle between fluid and surface. Based on the principal of operation of the droplet-shaped structures, we optimised the structure shape for better performance in targeted fluid flow and increase in flexibility in design of the structure geometry. To adapt the structure geometry and the structure spacing to the contact angle, we implemented an equilibrium simulation of the, the structure surrounding, fluid. In order to verify the functionality of the optimised structure, we designed and manufactured a prototype. By testing this prototype with pure water used as fluid, the functionality of the optimised structure and the simulation could be proved. This kind of structure may be used on technical surfaces where targeted fluid transport is needed, *e.g*. evacuation of condensate in order to prevent the surface from mold growth, microfluidics, lab-on-a-chip applications and on microneedles for efficient drug/vaccine coating.

Keywords: biomimetics, true bugs, liquid-surface interaction, passive unidirectional fluid transport, microfluidics, lab-on-a-chip

1 Introduction

In nature the interaction of fluids and surfaces is of major importance. Probably one of the best-known effects in connection with fluid surface interaction is the lotus effect[1–3]. Due to hierarchical wax structures on the leaf surface, the lotus leaf is superhydrophobic and therefore has excellent self-cleaning properties[4]. This self-cleaning property can be used in many technical applications[5], *e.g*. self-cleaning facade paint. Beside the lotus effect there are various other examples related to fluid surface interaction in nature, like the air retaining abilities of the *Salvinia molesta*[6]. The *Salvinia molesta* is able to retain an air film under water. This effect could be used for drag reduction on ships[6] or for oil spill clean-up in water[7]. In this paper the focus is on the effect of passive, unidirectional fluid transport[8,9], which can be observed in nature in some insects and reptiles. For example, the Texas horned lizard (*Phrynosoma cornutum*) covers part of its water demand by fog harvesting. Via their body surface they have access to water sources like fog, moist sand or dew. Through capillary systems the collected water is transported passive and unidirectional to the mouth[10–12]. Another example for passive, targeted fluid flow is the spermathecae (*receptaculum seminis*) of rabbit fleas (*Spilopsyllus cuniculi*) and rat fleas (*Xenopsylla cheopis*). In the spermathecae, female flea store sperm until suitable conditions to lay eggs are found. The spermathecae is a capillary system which is shaped in such a way to allow passive, unidirectional transportation of the stored sperm[13]. Some true bug species (*Pentatomidae*, *Cydnidae* and *Dysodius*) show droplet-shaped surface structures, which are part of their External Scent Efferent System (ESES). These structures generate a passive, unidirectional transportation of a defensive fluid, which protects the bugs against enemies, because they function as an open-capillary system[14–17]. Besides the examples already mentioned, there are various other examples in nature where the effect of passive unidirectional fluid transport can be observed, *e.g*. the back of desert beetles[18], spider silk[19], butterfly wings[20], cacti[21], bird beaks[22], the ventral

***Corresponding author:** Sebastian Lifka
E-mail: sebastian.lifka@jku.at

skin of the Arizona Mountain King Snake (*Lampropeltis pyromelana*)[23] and the peristome of pitcher plants[24–28]. With a look on biomimetics, the phenomenon of passive, unidirectional fluid transport is also interesting in terms of technical applications. For example, the surface structures of true bugs could be used on microneedles manufactured by means of laser engineering[29] for efficient drug/vaccine coating[30] or especially for microfluidics and lab-on-a-chip applications.

In this paper we take a closer look at the mechanism of passive, directed fluid transport found on true bugs[14]. In Fig. 1, Scanning Electron Microscopy (SEM) images obtained with a Philips 525 SEM (Philips, Germany), from the ESES of *Tritomegas bicolor* (*T. bicolor*) are depicted. One can see the spiky, ornamented structures which generate the passive, unidirectional fluid transport. In Fig. 2 an abstracted/simplified version of the structure is illustrated. One can see the fluid flow takes place only in one direction, because the fluid spreads differently at straight and curved areas of the structure shape[14].

The question is, if this structure, more precise the shape of a single structure unit cell, could be optimised with regard to increased performance in unidirectional fluid transport and in terms of more flexibility in design of the structure geometry. As the length and width of the droplet shaped structure found on bugs are related to each other, the targeted fluid flow of the droplet shaped structure works efficiently only at a certain aspect ratio (length: width)[14]. The main goal of the optimised structure is the possibility to design structure length and width independent from each other. Furthermore, to make use of these surface structures in technical applications, the geometry and the spacing between the structure unit cells must be adapted to the contact angle between the fluid and the surface. Therefore, the question is how the geometry and the structure spacing can be designed in such a way that a directed fluid flow in consideration of the contact angle is possible.

To answer these questions, we implemented an equilibrium simulation of the, the structure unit cell surrounding fluid, based on the mathematical formulation of the fluid surface described in the supplement of Ref. [14]. For optimisation of the structure shape, we extended the theory presented in Ref. [14] by concave structure curvature. Based on the mathematical theory and the working principal of this structure, we designed an optimised structure geometry with regard to good performance in unidirectional fluid flow and more flexibility in design, called the "Passive Equipotential Nature Inspired Structure". To verify the functionality of the optimised structure shape, we manufactured a prototype and tested the targeted fluid flow performance of the prototype with pure water.

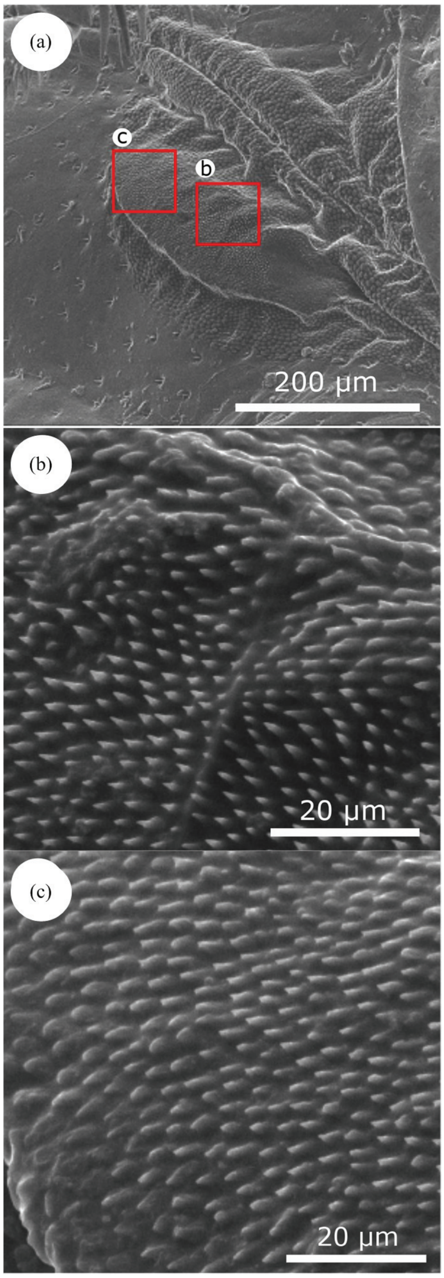

Fig. 1 (a) SEM overview from the ESES of *T. bicolor*. (b), (c) Magnified boxes from (a) showing the ornamented, spiky structures which generate the passive, unidirectional fluid transport.

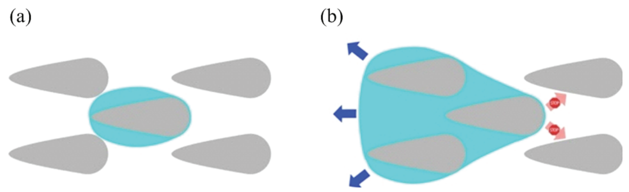

Fig. 2 Qualitative depiction of the series connection of the abstracted bug-structure unit cells. (a) The fluid flow around one unit cell spreads out wide at the straight areas, while the fluid is kept close at areas with strong curvature; (b) the fluid is able to reach the next iteration of unit cells to the left, whereas it is not able to reach the adjacent unit cells in the other direction, which leads to a unidirectional fluid transport.

2 Materials and methods

2.1 Optimisation

The droplet-shaped structure on the body surface of bugs works as an open-capillary system[14]. In areas with strong curvature of the structure shape the fluid front is kept close to the structure edge, whereas the fluid front spreads out wide in areas with weak or no curvature. In simple terms, the unidirectional fluid transport is obtained by putting a strong curved area of one unit cell opposite to a weak or non-curved area of adjacent unit cells. In one direction the fluid front is able to reach the next unit cell, but in the opposite direction the fluid does not reach the next unit cell. Therefore, the fluid flow is stopped in this direction. As long as there is fluid coming from a reservoir, the fluid front spreads from one structure unit cell to the other, but only in one direction.

With understanding of this mechanism, the droplet-shape of the structures found on bugs can be optimised. For good performance in terms of unidirectional fluid flow, the structure shape must contain a long, straight area where the fluid front can spread out to reach the next iteration of microstructures, in combination with a strong curved area on one end, in order to keep the fluid front close to the structure edge and therefore stop the flow in this direction. Fig. 3 shows the optimised shape of the structure geometry. It consists of a long straight area and two strong curved areas on each side on one end of the structure. In Fig. 3a the surrounding fluid is shown qualitative in blue. One can see that the fluid front spreads out at the straight area and is kept close to the edge at the strongly curved area. As shown in Fig. 3b, the fluid front at the straight area is able to reach the adjacent structure unit cells, whereas the fluid front at the curved areas is not able to reach the next iteration of structure unit cells. Therefore, the fluid front spreads out to the left, but stops to the right, as long as more fluid comes from a reservoir. Summarised, a passive, unidirectional fluid transport is achieved. In the following, this optimised structure is called "Passive Equipotential Nature Inspired Structure". In comparison to the droplet shaped structure, the length and the width of the Passive Equipotential Nature Inspired Structure can be chosen independent from each other. The transition from the straight to the curved part at the droplet shaped structure is a critical point in terms of unidirectional fluid transport. To ensure smooth transition, a certain aspect ratio must be maintained. As the Passive Equipotential Nature Inspired Structure consists of one long, straight part and two curved parts at one end, each part can be designed individually and independent from each other, which allows more flexibility in design of the structure geometry. Therefore, the Passive Equipotential Nature Inspired Structure can be theoretically adapted to almost every contact angle below 45° and above 10° (superhydrophilic). A key factor for good directed fluid transport is the spacing between the adjacent unit cells. The distance must be sufficient large to prevent the liquid from spreading into the wrong direction and sufficient small to ensure the fluid front reaches the next iteration of unit cells in spreading direction.

2.2 Extension of the mathematical theory describing the surrounding fluid surface

Compared to the droplet-shaped bug structure, the Passive Equipotential Nature Inspired Structure contains beside convex structure curvatures also concave curvatures. Therefore, the presented theory in Ref. [14] has to be extended by a mathematical representation of the fluid surface for concave structure curvatures. Connecting the local curvature H with the Laplace-pressure of liquids leads to

$$\Delta p = \frac{\partial E}{\partial V} = \gamma\left(\frac{1}{r_1} + \frac{1}{r_2}\right) = 2\gamma H, \quad (1)$$

where r_1 and r_2 are the main radii of curvature and γ is the surface tension of the liquid. Assume the liquid is connected to an infinite liquid reservoir at zero pressure and therefore is in a state of equilibrium, the fluid

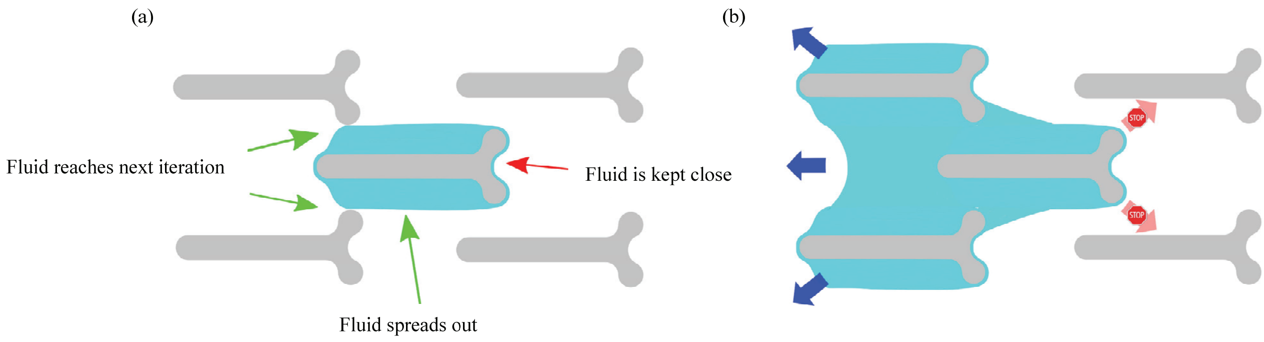

Fig. 3 Qualitative depiction of the series connection of Passive Equipotential Nature Inspired Structure unit cells. (a) The fluid flow around one unit cell spreads out wide at the straight areas, while the fluid is kept close at areas with strong curvature; (b) the fluid is able to reach the next iteration of unit cells to the left, whereas it is not able to reach the adjacent unit cells in the other direction, which leads to a unidirectional fluid transport.

surface forms a minimal surface which fulfils

$$\Delta p = 0 \Rightarrow H = 0 \Rightarrow \frac{1}{r_1} + \frac{1}{r_2} = 0. \tag{2}$$

For convex curvatures, in case of a right circular cylinder, the solution of the fluid surface surrounding the cylinder can be found to be a catenoid. A catenoid is a minimal surface which is obtained by rotating a catenary curve around an axis. This solution is only feasible for contact angles below 45˚. The exact position of the catenoid and therefore the position of the fluid surface surrounding the cylinder, can be determined by geometrical considerations based on the function of a catenary curve with regard to the boundary condition, namely the contact angle. The whole theory is presented detailed in the supplement of Ref. [14]. Basically, the same is done in the following, but this time for concave curvatures.

For concave curvatures of the structure, the solution of the fluid surface is also a catenoid. But, as a concave curvature has a negative sign compared to a convex curvature, the catenary curve describing the catenoid is rotated by 90˚. In Fig. 4 a concave, circular cylinder with the catenary curve in blue, with the z axis as rotation axis, is depicted. One must distinguish between three different cases. The first case is shown in Fig. 4, the catenary curve intersects the cylinder under the contact angle θ two times. The second case is depicted in Fig. 5, here the catenary curve is "fixed" on the top edge of the concave cylinder and intersects the cylinder bottom under the contact angle θ. This is the case if the radius R is too high or the height of the cylinder is too low. The third case occurs if the radius R is too low. In this case the cylinder is filled with fluid and the fluid surface forms a straight line at the top edge of the cylinder.

First, the case in Fig. 4 should be considered. To fit the catenary curve depending on the given parameters θ and R into the cylinder, the unknown parameters a, x_1, z_1 and z_2 must be calculated. The base function of a catenary curve is given by:

$$f(x) = a\cosh(\frac{x}{a}). \tag{3}$$

One can immediately write down the mathematical description for z_1 and z_2

$$z_1 = a\cosh(\frac{x_1}{a}), \tag{4}$$

$$z_2 = a\cosh(\frac{R}{a}). \tag{5}$$

The derivative of the catenary curve function is given by:

$$f'(x) = \sinh(\frac{x}{a}). \tag{6}$$

At $x = x_1$ the derivative of the catenary curve is $f'(x) = \tan\theta$ and at $x = R$ the derivative is $f'(x) = \cot\theta$. This leads to the following dependencies for x_1 and R

$$x_1 = a\sinh^{-1}(\tan\theta), \tag{7}$$

$$R = a\sinh^{-1}(\cot\theta). \tag{8}$$

Eq. (8) can be rewritten as:

$$a = \frac{R}{\sinh^{-1}(\cot\theta)}. \tag{9}$$

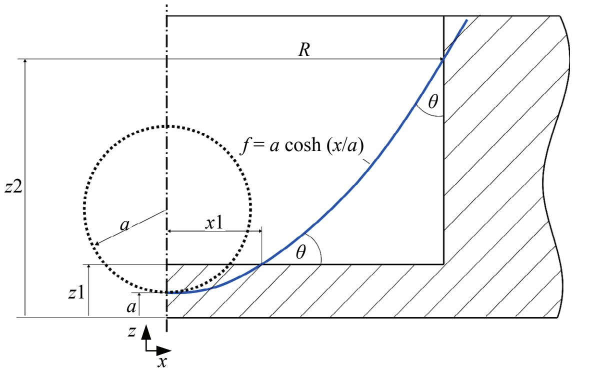

Fig. 4 Outline for the calculation of the catenary curve (blue) which intersects the cylinder two times under the contact angle θ.

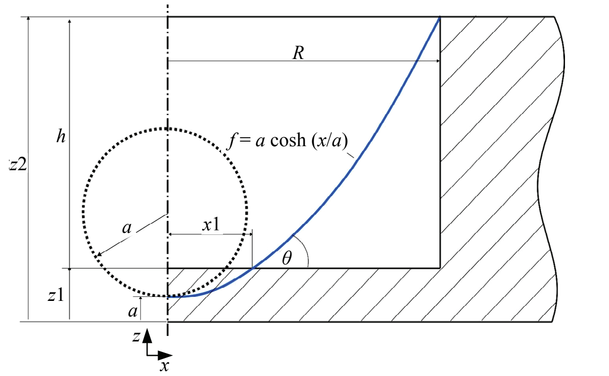

Fig. 5 Outline for the calculation of the catenary curve (blue) which intersects the cylinder at the bottom under the contact angle θ, while is fixed at the top edge, because the radius R is too high or the height h is too low.

Now four equations for the four unknown parameters, which determine the exact position of the catenary curve, are available.

For the second case, which occurs if the radius R is too high or the height h is too low, the catenary curve is "fixed" at the top edge of the cylinder in Fig. 5 and Eq. (8) is no longer valid. For z_2 the simple relationship

$$z_2 = a\cosh(\frac{R}{a}) = h + z_1, \tag{10}$$

can be written down. To get an equation for the parameter a, Eqs. (4) and (7) are inserted in Eq. (10). This leads to an implicit equation for a:

$$a = \frac{h}{\cosh(\frac{R}{a}) - \cosh(\sin^{-1}(\tan\theta))}, \tag{11}$$

which can be solved by iteration. Because the above mentioned third case is only a straight line on the top edge of the cylinder, no further calculations are necessary.

2.3 Simulation

Based on the theory presented in Ref. [14] and the extension of the theory presented above, the fluid flow around the structure unit cells can be simulated. Based on this simulation the structure dimensions and the spacing between the structure unit cells can be adapted to the contact angle, to ensure a unidirectional fluid flow. The underlying idea is to discretize the structure shape in a finite number of points (shape-points). At these points the structure shape is approximated as a right circular cylinder with a defined curvature. The curvature radius is calculated at every shape-point around the structure. To ensure steady curvature, the structure shape is interpolated with splines. Based on the contact angle, the structure height and the curvature radius, the resulting catenary curve at a defined shape-point can be calculated with the above presented theory. The catenary curves at all shape-points are connected to a surface which describes the fluid surface around the structure. The visualisation of this surface allows to adapt the structure dimensions and spacing to the contact angle. The simulation was implemented in MATLAB (The MathWorks, Inc., Natick, MA, USA; Version: R2017a) as follows.

First, the contact angle and the structure shape are defined. The x-y-coordinates of the shape are manually filled in an array and interpolated with the built in MATLAB-function spline(), which results in an array containing the shape-point-coordinates ($x_{\mathrm{sp,\ i}}$, $y_{\mathrm{sp,\ i}}$). In the next step the local curvature at the shape-points is calculated by building the first and second order derivative at these points. Because the coordinates of the interpolated shape are stored in an array, the derivatives can be calculated with the MATLAB-function diff(). The results are two arrays which contain the derivatives between the shape-points. To get the derivatives right at the shape-points, the slope differences between the two adjacent shape-points must be added together as follows (Fig. 6).

$$d_{x_i} = d_{x,i-1/i} + d_{x,i/i+1}, \tag{12}$$

$$d_{y_i} = d_{y,i-1/i} + d_{y,i/i+1}, \tag{13}$$

Now the local curvature κ can be calculated

$$\kappa = 2\frac{\dot{x}\ddot{y} - \ddot{x}\dot{y}}{(\dot{x}^2 + \dot{y}^2)^{3/2}}. \tag{14}$$

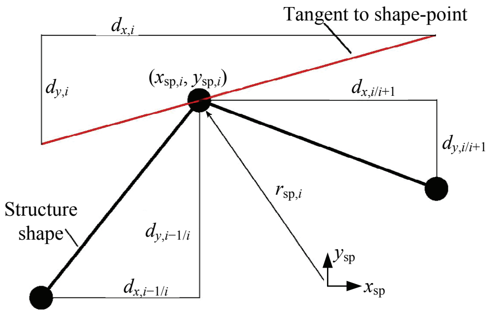

Fig. 6 Outline for the calculation of the tangent respectively the first derivative of the structure shape right at a shape-point. $d_{x,i-1/i}$ and $d_{x,i/i+1}$ describe the slope differences between the adjacent shape-points in x-direction, $d_{y,i-1/i}$ and $d_{y,i/i+1}$ describe the slope differences between the adjacent shape-points in y-direction. d_{x_i} and d_{y_i} are the sum of the slope differences in the respective direction and determine the tangent right at a shape-point. $(x_{sp,i}, y_{sp,i})$ are the coordinates of the current shape-point, with the position vector $\boldsymbol{r}_{sp,i}$.

By applying Eq. (14) directly on the arrays containing the derivatives, the local curvatures at the shape-points are obtained. To get the curvature radius R, which is necessary for the calculation of the catenary curves, the inverse of the curvature $R = 1/\kappa$ is formed. Once the radius R is known, the resulting catenary curves at the shape-points can be calculated. The catenary curves are represented by an array containing the x-z-coordinates, whereby the x-coordinate (x_{catenary}) stands for the distance from the structure edge and the z-coordinate (x_{catenary}) stands for the height.

In the last step the separate catenary curves are connected to a surface. Therefore, the catenary curves are attached orthogonal to the tangent at the shape-point. To do so, first the pitch angle of the tangent must be calculated as:

$$\alpha = \tan^{-1}\left(\frac{d_{y_i}}{d_{x_i}}\right). \tag{15}$$

Second the x-coordinates of the catenary curves must be corrected by the curvature radius R.

$$x_{\text{catenary,corr}} = \left|x_{\text{catenary}} - R\right|. \tag{16}$$

The correction by R is necessary, so that the coordinates of the catenary curve can be added to the coordinates of the structure shape (Fig. 7). The absolute value is necessary because with concave curvatures the radius R is greater than x_{catenary} (Fig. 5).

The x-y-coordinates of the fluid surface (x_{fluid}, y_{fluid}) are obtained by superposition of the x-y-shape-point-coordinates ($x_{\text{sp}}, y_{\text{sp}}$) with the corrected x-coordinates of the catenary curve-coordinates ($x_{\text{catenary, corr}}$) (Fig. 7)

$$x_{\text{fluid}} = x_{\text{sp}} \pm x_{\text{catenary,corr}} \sin\alpha, \tag{17}$$

$$y_{\text{fluid}} = y_{\text{sp}} \pm x_{\text{catenary,corr}} \cos\alpha. \tag{18}$$

The sign depends on the quadrant in which the respective shape-point is located.

2.4 Prototype

To test the functionality of the Passive Equipotential Nature Inspired Structure a prototype was manufactured. The prototype was made of a 2 mm thick polystyrene (PS) plate (Gutta Werke GmbH, Schutterwald, Germany). The contact angle of pure water on the PS-plate was measured with a custom-made contact angle measurement system according to the principle of drop shape analysis. The contact angle measurement resulted in a contact angle of $\theta = 84^\circ$. The used droplet volume was 2 µL. The outer dimensions of the prototype are 30 mm × 10 mm. The structure dimensions and spacing were designed for a contact angle of about 40°. Fig. 8 shows the detailed dimensions of the prototype. For test purposes only two rows of structures, which is necessary and sufficient for directed fluid flow, were fabricated.

The structures were manufactured by CNC-milling on a portal milling machine PRO-BASIC-H 06/05 (CNC-Modellbau, Gerabronn, Germany) with a 3S Step-control (CNC-Modellbau, Gerabronn, Germany) and a Kress 800 FME milling spindle (KRESS-elektrik GmbH & Co. KG, Bisingen, Germany), which was controlled via the software WinPC-NC USB (Burkhard Lewetz Hard- und Software, Meckenbeuren, Germany; Version: 2.50/20). For the small microstructures a 0.3 mm right-hand cutting solid carbide single tooth cutter (Karnasch Professional Tools GmbH, Heddesheim, Germany; Item number: 29 1652) was used. For face-milling a 6 mm double-edged, titanium coated end mill (Paulitschek Maschinen- und Warenvertriebsgesellschaft mbH, Neu-Ulm, Germany; Item number: 13001) and for cutting out the outer contours a 1 mm double-edged, HSS-E CO5 end mill (Paulitschek Maschinen- und Warenvertriebsgesellschaft mbH, Neu-Ulm, Germany; Item number: 13350) was used.

The speed of the cutter was set to the lowest available value of 10000 rpm in order to prevent the PS from melting. The infeed for the 0.3 mm micro-cutter was 0.1 mm and for the other cutters 0.25 mm. The used cutting data are listed in Table 1. The CAD-data was

Table 1 Cutting data (mm·min^{-1}) for the cutter diameters used

	Cutting feed	Retraction feed	Extension feed	Helix feed	Plunging feed-rate
0.3 mm cutter	120	80	80	50	50
1 mm cutter	150	80	80	50	50
6 mm cutter	300	100	100	80	80

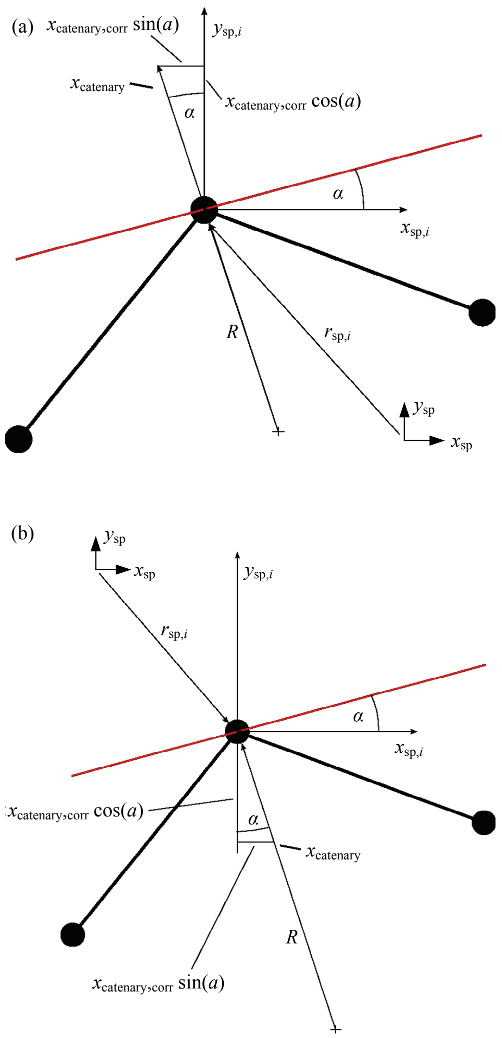

Fig. 7 Outline for the superposition of the shape-point-coordinates with the catenary curve-coordinates. The curvature radius R has to be subtracted from the x-catenary curve-coordinates to transform the x-catenary curve-coordinates into the local coordinate system of the current shape point ($x_{\text{sp},i}$, $y_{\text{sp},i}$). (a) shows a convex curvature, while (b) shows a concave curvature.

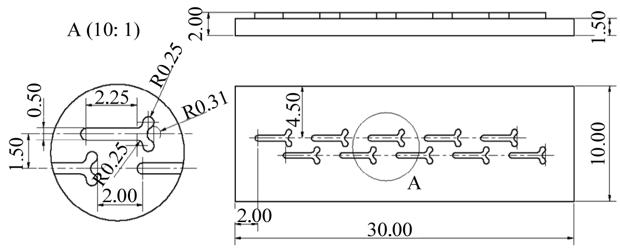

Fig. 8 Construction drawing for the prototype of the Passive Equipotential Nature Inspired Structure (dimensions in mm). The structure dimensions and spacing was designed for a contact angle of about 40°. Two rows of structures are necessary and sufficient for passive, unidirectional fluid flow.

created in Autodesk Inventor (Autodesk, Inc., San Rafael, CA, USA; Version: Inventor 2019) and the G-code for the CNC-machine was created with Autodesk Fusion 360 (Autodesk, Inc., San Rafael, CA, USA; Version: 2.0.8412).

After the milling process, the surface of the prototype was smoothed with vaporous chloroform in order to prevent the fluid from getting stuck at surface irregularities due to the milling process. The structured prototype was therefore put in a desiccator together with a small Petri dish filled with chloroform. The desiccator was then evacuated and after about 30 min, the prototype was taken out of the desiccator.

To make the prototype, made of PS, work with pure water, the contact angle has to be reduced below 45°, because otherwise the directed fluid flow with the Passive Equipotential Nature Inspired Structure does not work. This was achieved by hydrophilizing the PS with an UV/Ozone-treatment. Therefore, the prototype was treated by means of a UV-excimer-lamp (Excimer-VG, Heraeus Noblelight GmbH, Hanau, Germany) with a wavelength of 172 nm and a pressure of 5 mbar for 15 min. After the treatment, the PS showed a contact angle of about 40° with pure water, which is sufficient for the Passive Equipotential Nature Inspired Structure.

The fluid flow was tested with pure water which was dyed red with Ponceau S (C.J. 27195) (Carl Roth GmbH & Co. KG, Karlsruhe, Germany) to enhance visibility. Previous investigations have shown that Ponceau S (C.J. 27195) does not affect the contact angle. The water was applied with a pipette and the amount was chosen individually. To record the results of the fluid flow, videos were recorded by means of a video camera and post processed with DaVinci Resolve (Blackmagic Design Pty. Ltd, Fremont, CA, USA; Version: 16.2.2.012).

3 Results

3.1 Simulation

In the following illustrations the results of the simulations for different structure shapes are depicted. Fig. 9 shows the droplet-shaped bug-structure found on true bugs, simulated with two different contact angles. In Fig. 10 the Passive Equipotential Nature Inspired Structure is depicted, also with two different contact angles. One can see the different spreading behaviour of the fluid, resulting from different contact angles. The lower the contact angle, the wider the fluid spreads out. The simulation also shows that the fluid spreads out wide at areas with low curvature and is kept close to the structure edge at areas with high curvature. In stop-direction, the fluid at the Passive Equipotential Nature Inspired Structure is, in contrast to the bug-structure, clearly kept closer to the structure edge, which results in better performance in directed fluid flow.

3.2 Prototype and directed fluid flow

In Fig. 11 an image sequence of the directed fluid flow with the prototype described in section **2.4** is depicted (the full video is available in supplementary materials, video 1). One can see the fluid front spreading out to the left as expected, whereas stopping to the right. In Fig. 12 an image sequence of an up-scaled prototype, in order to enhance the visibility of the fluid flow around single structure unit cells, is depicted (the full video is available in supplementary materials, video 2). One can see the fluid spreading out to the left, whereas stopping to the right. Due to the up scaling of the structure dimensions, the spreading velocity of the second prototype is lower than the velocity of the first prototype. Besides the spread to the left one can see wetting and fluid transport to the right. This is because the initial unit cell where the droplet was applied is filled up until it is completely surrounded by the fluid. The distance which the fluid is transported in the opposite direction depends on the size of the unit cells, the smaller one unit cell, the shorter the transport distance in the other direction.

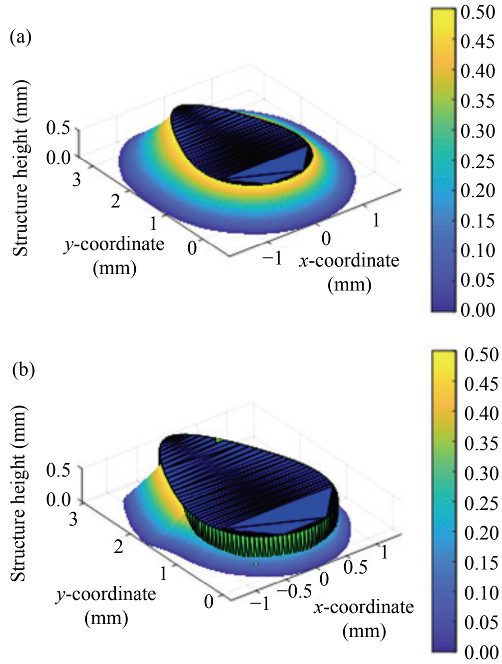

Fig. 9 Simulation of the fluid flow around the droplet-shaped bug-structure with different contact angles. (a) Birds eye view with a contact angle of $\theta = 25^\circ$; (b) birds eye view with a contact angle of $\theta = 40^\circ$. The fluid spreads out differently depending on the contact angle. At low curvature areas the fluid spreads out wider than at strong curvature areas.

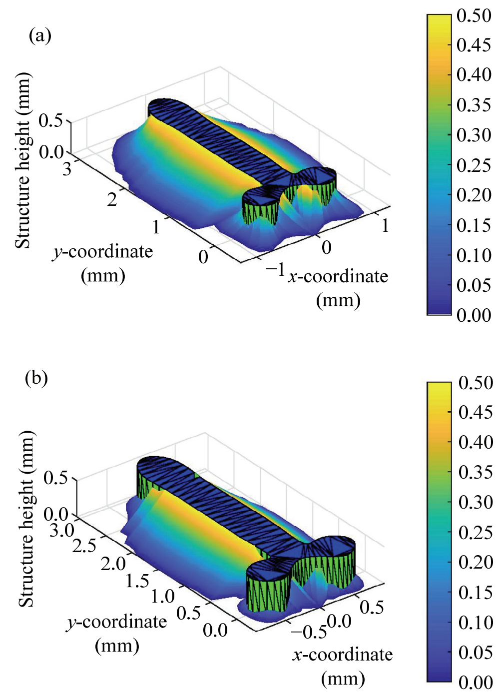

Fig. 10 Simulation of the fluid flow around the Passive Equipotential Nature Inspired Structure with different contact angles. (a) Birds eye view with a contact angle of $\theta = 25^\circ$; (b) birds eye view with a contact angle of $\theta = 40^\circ$. The fluid spreads out differently depending on the contact angle. At low curvature areas the fluid spreads out wider than at strong curvature areas.

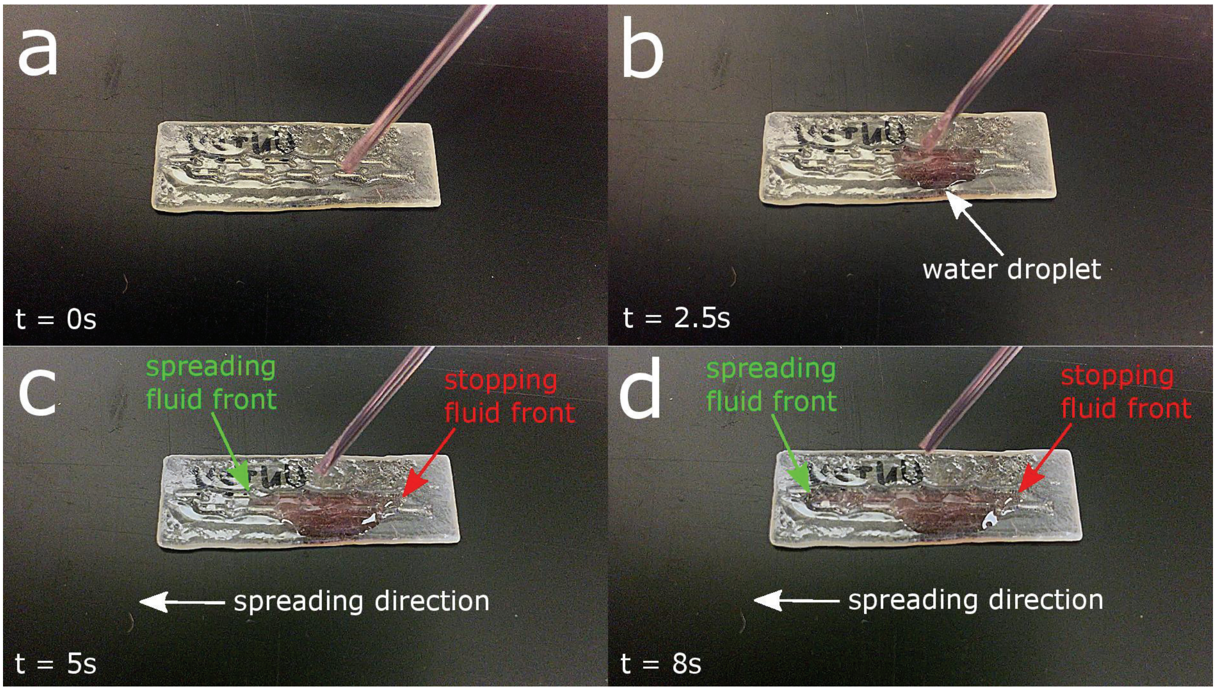

Fig. 11 Image sequence of the unidirectional fluid flow with the prototype of the Passive Equipotential Nature Inspired Structure described in section **2.4**. One can see the fluid front spreading out to the left in forward-direction, whereas stopping to the right in stop-direction. (a) Prototype; (b) A water droplet is placed on the prototype with a pipette; (c)–(d) The fluid spreads out to the left, whereas stops to the right. Besides the spread to the left one can see wetting and fluid transport to the right. This is because the initial unit cell where the droplet was applied is filled up until it is completely surrounded by the fluid.

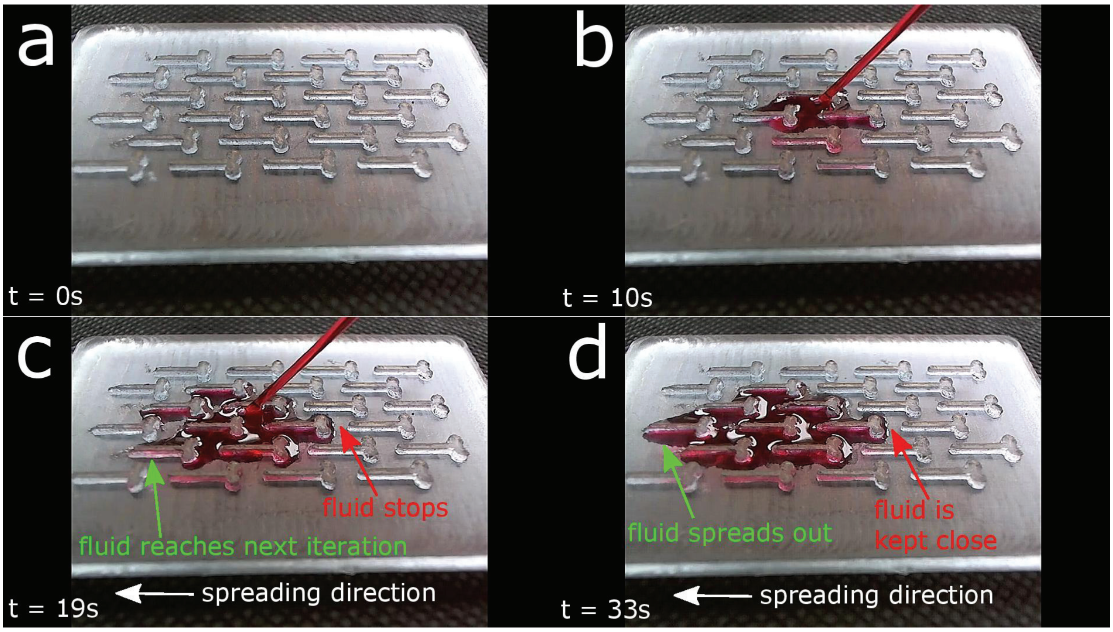

Fig. 12 Image sequence of the unidirectional fluid flow with an up-scaled prototype of the Passive Equipotential Nature Inspired Structure. One can see the fluid front spreading out to the left in forward-direction, whereas stopping to the right in stop-direction. (a) Up-scaled prototype; (b) a water droplet is placed on the prototype with a pipette; (c) the fluid flows around the single structure unit cells similar to the simulations presented in section **2.3**. The fluid reaches the next iteration to the left, whereas stops to the right; (d) the fluid spreads further to the left and is kept close to the structure edge in the other direction. Besides the spread to the left one can see wetting and fluid transport to the right. This is because the initial unit cell where the droplet was applied is filled up until it is completely surrounded by the fluid.

4 Discussion

Droplet-shaped structures, which are part of the ESES of some true bug species, generate a passive, unidirectional fluid flow. With knowledge of the functional principal of these droplet-shaped structures, the shape could be optimised with regard to better performance in unidirectional fluid transport. Due to the fact that these sublime structures work as an open-capillary system and that the fluid front spreads out differently depending on the curvature of the structure shape, an optimised shape, the so called "Passive Equipotential Nature Inspired Structure", was implemented. The main advantage of the Passive Equipotential Nature Inspired Structure compared to the droplet shaped structure found on true bugs is the higher flexibility in design of the structure geometry, because at the Passive Equipotential Nature Inspired Structure no certain aspect ratio has to be maintained. A direct comparison with the droplet shaped structure from Ref. [14] is difficult to achieve, as the size ratios are different (mm for the Passive Equipotential Nature Inspired Structure and µm for the droplet shaped structure). At the moment were not yet able to produce the Passive Equipotential Nature Inspired Structure as small as the droplet shaped structure. The other issue of interest, namely how the structure dimensions and the spacing between the structure unit cells can be adapted to the contact angle, was tackled with an equilibrium simulation of the, the structure surrounding, fluid. By visualising the fluid surface around the structure, the spacing between the structures can be designed to be suitable for the contact angle.

It has to be emphasised that the simulation of the fluid surface is more or less a qualitative representation. These simulations help to adapt the structure spacing to the contact angle by checking how far the fluid front spreads out maximally at the straight areas and minimally at the areas with high curvature. The simulation does not claim to fully reflect the real behaviour of the fluid flowing around the structure. For example, gravity is not considered in the simulation. Besides that, due to the separate calculation of the single catenary curves at the shape-points it can occur, that single catenary curves intersect each other in areas with concave curvature. In reality this would lead to a surface which is slightly different from the presented theory but is not considered in the simulation. Another point where the simulation differs from reality, are rapid changes in fluid-height at areas with high change in curvature.

Tests with the prototype showed, that the Passive Equipotential Nature Inspired Structure allows an effective passive, unidirectional fluid flow. After hydrophilizing the PS, the contact angle of pure water on the PS was 40˚. The maximal contact angle at which the Passive Equipotential Nature Inspired Structure works is 45˚. This means that the contact angle of the prototype is very close to the maximum allowed contact angle, which leads to a low velocity of propagation of the fluid front and causes the fluid front to get stuck easily at surface irregularities. This problem may be overcome by using other materials or fluids with lower surface tension than pure water, *e.g.* soapy water. The combination of PS and pure water was chosen, because on the one hand PS is easy to handle, especially for milling with very thin and fragile 0.3 mm micro cutters. On the other hand, it has been proven, that these kinds of structures also work with pure water and not only with soapy water or oil, as it was used in the experimental of Refs. [13–15].

These structures may be used for a broad spectrum of technical applications where it comes to fluid surface interaction. For example, the Passive Equipotential Nature Inspired Structure could be used to drain off condensate from surfaces to protect the surface from mold growth. This scenario appears *e.g.* on the plates of plate heat exchangers used in ventilation systems of modern buildings, especially during the winter months, where cold and dry air is exchanged with warm and high humidity air. Further possible applications are structured surfaces for coolant transportation, structured diaper inlays which help to spread the fluid to ensure even absorption and innovative structured microneedles for efficient drug/vaccine coating[30]. Besides that, the field of microfluidics and lab-on-a-chip applications seem to be a suitable target for the presented structure.

Furthermore, another possible extension for the usage of the Passive Equipotential Nature Inspired Structure and similar structures may be the combination with the effect of electro wetting[31]. An electric field affects the surface tension of a liquid which leads to a better wetting behaviour and therefore to lower contact angles. For example, the structure could be designed in such a way, that at zero electric field no flow takes place. If an electric field is applied, the contact angle is lowered, which leads to a passive, unidirectional fluid flow. If the electric field is increased, the contact angle gets even lower until a fluid flow in both directions is achieved. Therefore, a voltage-controlled fluid flow may be implemented, which is especially of interest for applications in the field of microfluidics.

5 Conclusion

With the Passive Equipotential Nature Inspired Structure, a further developed structure shape for passive, unidirectional fluid transport was introduced and verified in functionality with a CNC-milled prototype made of PS. To facilitate the design of the dimensions and spacing of the structures, an equilibrium simulation was implemented. By qualitative simulation of the fluid surface around the structure unit cells depending on the contact angle, one can adapt the structure spacing and dimension. In future works the Passive Equipotential Nature Inspired Structure may be manufactured by means of 3D-printing, *e. g*. Selective Laser Sintering (SLS). The advantage of this manufacturing process is on the one hand the easy way of production without the need of fragile micro cutters and with zero material waste. On the other hand, SLS possibly opens up, due to the powder-based process, an easy way of hydrophilization by adding hydrophilic additives, *e.g*. metallic particles or glass beads, to the powder.

Acknowledgment

This work was supported by the European Union's Horizon 2020 research and innovation program within the project "BioComb4Nanofibers" (grant agreement No. 862016) and the Linz Center of Mechatronics (LCM).

* All supplementary materials are available at https://doi.org/10.1007/s42235-021-0027-x.

References

[1] Barthlott W, Neinhuis C. Purity of the sacred lotus, or escape from contamination in biological surfaces. *Planta*, 1997, **202**, 1–8.

[2] Marmur A. The lotus effect: Superhydrophobicity and metastability. *Langmuir*, 2004, **20**, 3517–3519.

[3] Ensikat H J, Ditsche-Kuru P, Neinhuis C, Barthlott W. Superhydrophobicity in perfection: The outstanding properties of the lotus leaf. *Beilstein Journal of Nanotechnology*, 2011, **2**, 152–161.

[4] Bhushan B, Koch K, Jung Y C. Biomimetic hierarchical structure for self-cleaning. *Applied Physics Letter*, 2008, **93**, 093101.

[5] Spaeth M, Barthlott W. Lotus-effect®: Biomimetic super-hydrophobic surfaces and their application. *Advances in Science and Technology*, 2008, **60**, 38–46.

[6] Barthlott W, Schimmel T, Wiersch S, Koch K, Brede M, Barczewski M, Walheim S, Weis A, Kaltenmaier A, Leder A, Bohn H F. The *salvinia* paradox: Superhydrophobic surfaces with hydrophobic pins for air retention under water. *Advanced Materials*, 2010, **22**, 2325–2328.

[7] Zeiger C, Rodrigues da Silva I C, Mail M, Kavalenka M N, Barthlott W, Holscher H. Microstructures of superhydrophobic plant leaves – inspiration for efficient oil spill cleanup materials. *Bioinspiratoin* & *Biomimetics*, 2016, **11**, 056003.

[8] Li J Q, Zhou X F, Li J, Che L F, Yao J, McHale G, Chaudhury M K, Wang Z K. Topological liquid diode. *Science Advances*, 2017, **3**, eaao3530.

[9] Liu C R, Sun J, Li J, Xiang C H, Che L F, Wang Z K, Zhou X F. Long-range spontaneous self-propulsion on wettability gradient surfaces. *Scientific Reports*, 2017, **7**, 7552.

[10] Comanns P, Buchberger G, Buchsbaum A, Baumgartner R,

Kogler A, Bauer S, Baumgartner W. Directional, passive liquid transport: The Texas horned lizard as a model for a biomimetic "liquid diode". *Journal of the Royal Society Interface*, 2015, **12**, 20150415.

[11] Comanns P, Effertz C, Hischen F, Staudt K, Böhme W, Baumgartner W. Moisture harvesting and water transport through specialized micro-structures on the integument of lizards. *Beilstein Journal of Nanotechnology*, 2011, **2**, 204–214.

[12] Buchberger G, Hischen F, Comanns P, Baumgartner R, Kogler A, Buchsbaum A, Bauer S, Baumgartner W. Bio-inspired microfluidic devices for passive, directional liquid transport: Model-based adaption for different materials. *Procedia Engineering*, 2015, **120**, 106–111.

[13] Buchberger G, Kogler A, Weth A, Baumgartner R, Comanns P, Bauer S, Baumgartner W. "Fluidic Diode" for passive unidirectional liquid transport bioinspired by the spermathecae of fleas. *Journal of Bionic Engineering*, 2018, **15**, 42–56.

[14] Hischen F, Buchberger G, Plamadeala C, Armbruster O, Heiss E, Winands K, Schwarz M, Jüttler B, Heitz J, Baumgartner W. The external scent efferent system of selected European true bugs (Heteroptera): A biomimetic inspiration for passive, unidirectional fluid transport. *Journal of The Royal Society Interface*, 2018, **15**, 20170975.

[15] Plamadeala C, Hischen F, Friesenecker R, Wollhofen R, Jacak J, Buchberger G, Heiss E, Klar T A, Baumgartner W, Heitz J. Bioinspired polymer microstructures for directional transport of oily liquids. *Royal Society Open Science*, 2017, **4**, 160849.

[16] Kirner S V, Hermens U, Mimidis A, Skoulas E, Florian C, Hischen F, Plamadeala C, Baumgartner W, Winands K, Mescheder H, Krüger J, Solis J, Siegel J, Stratakis E, Bonse J. Mimicking bug-like surface structures and their fluid transport produced by ultrashort laser pulse irradiation of steel. *Applied Physics A*, 2017, **123**, 754.

[17] Krall B S, Bartelt R J, Lewis C J. Chemical defense in the stink bug cosmopepla bimaculate. *Journal of Chemical Ecology*, 1999, **25**, 2477–2494.

[18] Parker A, Lawrence C. Water capture by a desert beetle. *Nature*, 2001, **414**, 33–34.

[19] Zheng Y, Bai H, Huang Z, Tian X, Nie F Q, Zhao Y, Zhai J, Jiang L. Directional water collection on wetted spider silk. *Nature*, 2010, **463**, 640–643.

[20] Liu C, Ju J, Zheng Y, Jiang L. Asymmetric ratchet effect for directional transport of fog drops on static and dynamic butterfly wings. *ACS Nano*, 2014, **8**, 1321–1329.

[21] Ju J, Bai H, Zheng Y, Zhao T, Fang R, Jiang L. A multi-structural and multi-functional integrated fog collection system in cactus. *Nature Communications*, 2012, **3**, 1247.

[22] Prakash M, Quéré D, Bush J W M. Surface tension transport of prey by feeding shorebirds: The capillary ratchet. *Science*, 2008, **320**, 931–934.

[23] Tenjimbayashi M, Kawamura K, Shiratori S. Continuous directional water transport on hydrophobis slippery ventral skin of lampropeltis pyromelana. *Advanced Materials Interfaces*, 2020, **7**, 2000984.

[24] Chen H W, Zhang P F, Zhang L W, Liu H L, Jiang Y, Zhang D Y, Han Z W, Jiang L. Continuous directional water transport on the peristome surface of *Nepenthes alata*. *Nature*, 2016, **532**, 85–89.

[25] Li J, Guo Z G. Spontaneous directional transportations of water droplets on surfaces driven by gradient structures. *Nanoscale*, 2018, **10**, 13814–13831.

[26] Sun W X, Tang L J, Hong W, Zhan Y J, Yang B, Liu J Q. A novel microstructure inspired from *Nepenthes alata* and lizard skin and its enhanced uni-directional liquid spreading property. *RSC Advances*, 2019, **9**, 7842–7848.

[27] Li X, Li J Q, Dong G N. Bioinspired topological surface for directional oil lubrication. *ACS Applied Materials* & *Interfaces*, 2020, **12**, 5113–5119.

[28] Li J Q, Zheng H X, Yang Z B, Wang Z K. Breakdown in the directional transport of droplets on the peristome of pitcher plants. *Communication Physics*, 2018, **1**, 35.

[29] Stratakis E, Bonse J, Heitz J, Siegel J, Tsibidis G D, Skoulas E, Papadopoulos A, Mimidis A, Joel A C, Comanns P, Krüger J, Florian C, Fuentes-Edfuf Y, Solis J, Baumgartner W. Laser engineering of biomimetic surfaces. *Materials Science and Engineering*: *R*: *Reports*, 220, **141**, 100562.

[30] Plamadeala C, Gosain S R, Hischen F, Buchroithner B, Puthukodan S, Jacak J, Bocchino A, Whelan D, O'Mahony C, Baumgartner W, Heitz J. Bio-inspired microneedle design for efficient drug/vaccine coating. *Biomedical Microdevices*, 2020, **22**, 8.

[31] Mugele F, Baret J C. Electrowetting: From basics to applications. *Journal of Physics*: *Condensed Matter*, 2005, **17**, R705–R774.